A navigation method for targeted prostate biopsy based on MRI-TRUS fusion

HU Jisu[1, 2] , MA Qi[3] , QIAN Xusheng[1, 2] , ZHOU Zhiyong[2, 4] , DAI Yakang[2, 4]

(1. School of Biomedical Engineering (Suzhou) , University of Science and Technology of China, Suzhou 215163, China; 2 Suzhou Institute of Biomedical Engineering and Technology, Chinese Academy of Sciences, Suzhou 215163, China; 3 Second Affiliated Hospital of Suzhou University, Suzhou 215000, China; 4Jinan Guoke Medical Engineering Technology Development Company, Ltd. , Jinan, Shandong 250000, China)

Abstract: A navigation method is proposed to enable the fusion of magnetic resonance imaging (MRI) and transrectal ultrasound (TRUS) for targeted prostate biopsy. This method directly establishes the transfor-mation between the preoperative MRI image and the intraoperative TRUS based on the selected coplanar MRI and TRUS images without the use of 3D TRUS. According to the real-time spatial pose of the intrao-perative TRUS, the resliced preoperative MRI image is computed and displayed along with the preoperative planning 3D model, and the planned lesion region is mapped to TRUS to guide the needle in-sertion. In the phantom experiment, the average error between the planned target point and the actual puncture position was calculated to be (1.98±0.28) mm. The experimental results show that this method can achieve high targeting accuracy and has potential value in clinical applications.

Keywords: Prostate cancer; Prostate biopsy; Magnetic resonance imaging; Transrectal ultrasound; Electromagnetic tracking

CLC No.: R 318   Document identification code: A

0 Introduction

Transrectal ultrasound (TRUS) -guided prostate biopsy is still the gold standard for clinical diagnosis of prostate cancer. However, due to low TRUS spatial resolution and poor imaging contrast, prostate cancer lesions are often difficult to identify or even invisible. Therefore, the prostate is usually divided into multiple areas of equal volume for 10~12 needle systematic biopsy [1-3]. Nevertheless, clinicians are still likely to miss the target lesion, resulting in repeated puncture, which will bring additional pain and cost to patients. On the other hand, magnetic resonance imaging (MRI) has become an important diagnostic technique for prostate cancer [1-3]. Compared with trus, MRI has higher spatial resolution and provides a variety of imaging contrast, which can greatly help clinicians detect target lesions and further judge their malignancy. However, the MRI imaging speed is too slow. More importantly, all biopsy

equipment must be compatible with the high field environment, which limits the popularization and application of MRI guided prostate biopsy.

In order to combine the advantages of MRI and trus, the fusion of preoperative MRI and intraoperative TRUS is the most common method for prostate targeted puncture. This research is mainly divided into MRI-TRUS registration method [4-7] and targeted puncture system construction [8-11]. The gray difference between TRUS and MRI images and the deformation of prostate due to the compression of probe have always been the key and difficult points in the research of prostate MRI-TRUS registration method. Many scholars [4-6] have integrated shape statistical model, biomechanical model and finite element analysis into traditional registration methods to achieve high-precision 3D trus-mri elastic registration, but the calculation process is complex and time-consuming. In recent years, Hu et al. [7] proposed an mri-3d TRUS registration method based on weak supervised in-depth learning. Fast and accurate elastic registration can be achieved based on weak labeling of prostate segmentation areas in MRI and 3D TRUS. However, both the traditional registration method and the registration method based on deep learning need to accurately segment the prostate region in TRUS and MRI. Especially for the prostate segmentation of TRUS, the noise and artifacts in TRUS will greatly affect the accuracy and stability of segmentation results, and then affect the practical application effect of these registration methods. Another kind of research mainly focuses on the construction method of targeted puncture system. Although this kind of research adopts a relatively simple registration method, it also achieves better targeted puncture accuracy

and has more clinical application value. As early as 2008, Xu et al. [8] proposed a targeted puncture guidance system based on electromagnetic positioning, which established the conversion relationship between preoperative MRI and real-time two-dimensional ultrasound in the book by manually scanning the three-dimensional reconstruction image of two-dimensional ultrasound through free arm three-dimensional ultrasound. However, manually scanning two-dimensional ultrasound is easy to affect the accuracy of three-dimensional reconstruction, thus affecting the fusion accuracy of ultrasound and magnetic resonance images. For this reason, many scholars [9-11] directly selected the three-dimensional ultrasonic probe to replace the free arm three-dimensional ultrasound, and achieved better puncture accuracy. However, these methods all use three-dimensional ultrasound as an intermediary to establish the relationship between preoperative MRI and intraoperative 2D TRUS. At present, three-dimensional ultrasound probes are only equipped in a few high-end models and have not been widely used. Therefore, this study will directly establish the spatial relationship between preoperative MRI and intraoperative 2D TRUS to achieve targeted prostate puncture guidance.

In this study, the electromagnetic positioning technology is used to obtain the spatial pose of 2D TRUS. Without using 3D TRUS data, the selected MRI level is rigidly registered with 2D TRUS based on mutual information measure, and then the spatial conversion relationship between preoperative MRI images and intraoperative 2D TRUS images is established. According to the real-time spatial pose of TRUS during the operation, the preoperative MRI re section was made. By observing the relative position relationship

between the re section image and the preoperative planning 3D visualization model, and mapping the preoperative planning focus area into trus, the puncture and needle insertion were guided to achieve accurate prostate targeted puncture guidance. In this study, a biplane intracavitary ultrasound probe was used to realize the whole targeted puncture guidance process for transperineal puncture, and the prostate phantom was used for experimental verification.

1 Method

This method directly establishes the conversion relationship between intraoperative 2D TRUS and preoperative MRI images, $\boldsymbol{m} = \boldsymbol{T}_{m \neg w} \boldsymbol{T}_{w \neg s} \boldsymbol{T}_{s \neg u} \boldsymbol{u}$, where $\boldsymbol{u} = [x_u, y_u, 0, 1]^{\mathrm{T}}$

and $\boldsymbol{m} = [x_m, y_m, z_m, 1]^{\mathrm{T}}$ are the coordinate points under TRUS coordinate system and MRI coordinate system respectively, $\boldsymbol{T}_{s \neg u}$ is the transformation matrix from TRUS coordinate system to magnetic positioning sensor coordinate system, which is calculated by ultrasonic probe calibration method, and $\boldsymbol{T}_{w \neg s}$ is the transformation matrix from magnetic positioning sensor coordinate system to magnetic positioning spatial coordinate system, Directly obtained from the degree of magnetic positioning sensor, $\boldsymbol{T}_{m \neg w}$ is the transformation matrix from magnetic positioning spatial coordinate system to MRI image spatial coordinate system, which is calculated by the semi-automatic image registration method proposed in this paper. This method does not need to establish the conversion relationship between 2D TRUS and MRI through 3D TRUS,

but directly establishes the conversion relationship between 2D TRUS and 3D MRI image space by selecting the same plane TRUS and MRI level for two-dimensional registration in a semi-automatic manner. During puncture guidance, the target area determined by preoperative MRI is mapped into trus, and the preoperative MRI image is re sectioned according to the real-time spatial position of TRUS. The ultrasonic imaging position is determined by observing the position relationship between the three-dimensional model of prostate and the real-time re sectioned MRI image, and the appropriate puncture path is selected in the special puncture fixture according to the distance between the focus and the ultrasonic probe to realize the guidance of prostate targeted puncture.
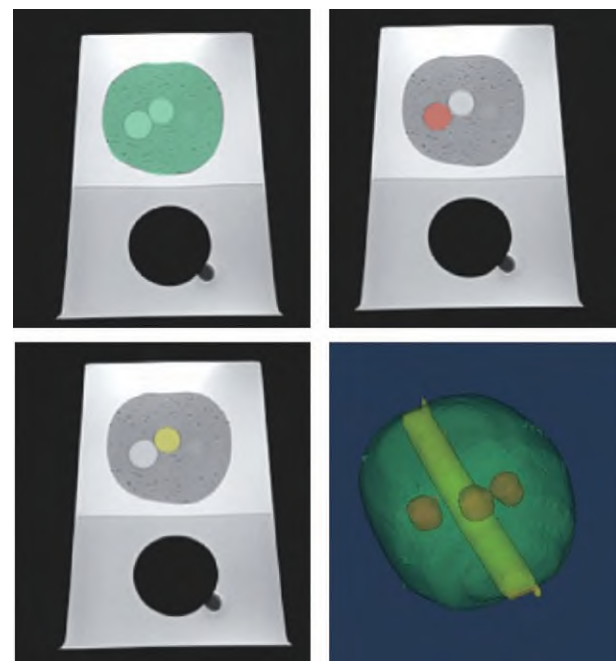

Figure 1 Prostate gland, focus, urethral segmentation area and three-dimensional model of prostate phantom

1.1 Preoperative planning

Firstly, the prostate, urethra and focus area are segmented according to the preoperative MRI image. The prostate area is automatically

segmented using the pre trained vnet[12] convolution neural network, and the urethra and focus area are manually delineated layer by layer. For patient images, the focus area needs to be comprehensively determined in combination with T2W and DWI high b-value images. At this time, the focus needs to be outlined under the joint display of T2W and DWI. Finally, we generate a three-dimensional model of the prostate, urethra and lesion area according to the segmentation results, which can help doctors observe the location of the lesion in the three-dimensional space of the prostate.

1.2 Ultrasonic calibration

In order to determine the position and attitude of TRUS image in three-dimensional space, we fix the magnetic positioning sensor on the ultrasonic probe through the probe clamp [Figure 2 (a)] and indirectly obtain the position of the ultrasonic image with the help of the magnetic positioning sensor. Therefore, it is necessary to calibrate the transformation matrix

$T_{s \neg u}$ [13] from the ultrasonic image coordinate

system to the magnetic positioning receiver coordinate system. According to the n-like line calibration principle, we designed the special calibration simulator shown in Figure 2 (b), and its wiring mode between two parallel plates is shown as the black solid line in Figure 2 (c). Several positioning holes are designed on the top of the simulation. The coordinates of the positioning holes in the magnetic positioning transmitter coordinate system can be obtained by using the magnetic positioning probe pen, and then the magnetic positioning space coordinates of all the line holes (such as W_1 and $W2$) can be deduced according to the mechanical design parameters, and then the magnetic positioning space coordinates of the virtual n-

line vertex (such as $W_1\mathcal{C}$ and $W_2\mathcal{C}$) can be deduced. When the ultrasonic probe is used to scan the phantom, the intersection of the ultrasonic imaging plane and the phantom line will form a grid point image, and each line of grid points corresponds to the intersection of the image plane and a layer of n-line structure. For every three adjacent image points along the line (such as U_1, U_2 and U_3), set the magnetic positioning spatial coordinate of the intersection point corresponding to U_2 as W, and obtain W according to the properties

$W_2\mathcal{C}W / WW_1\mathcal{C} = U_1U_2 / U_2U_3$ of similar triangles.

According to this, the point set u of several intersection points in TRUS image coordinate system and the corresponding point set in magnetic positioning space coordinate system w

can be obtained. According to $w = T_{w \neg s} T_{s \neg u} u$,

the point set $T_{w \neg s}$ is obtained from the data of

magnetic positioning sensor, and finally $T_{s \neg u}$

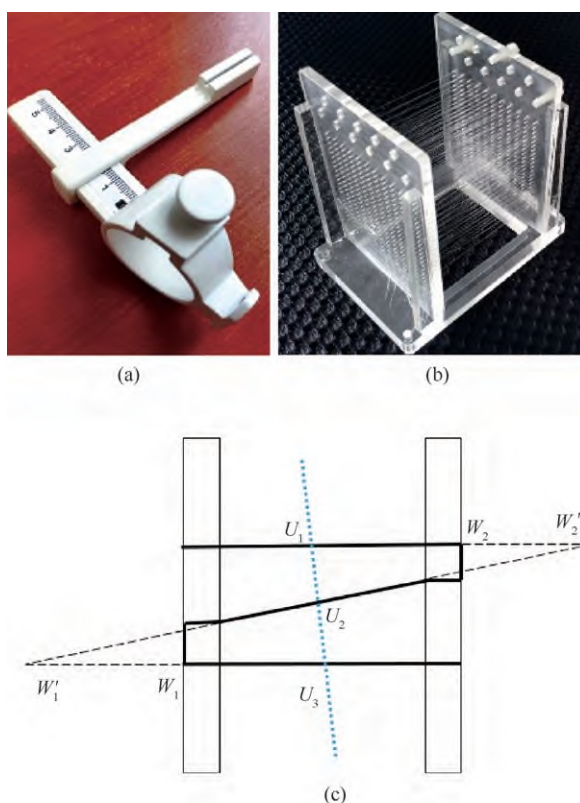is obtained by singular value decomposition method [14].

Figure 2 Schematic diagram of probe fixture,
calibration phantom and calibration principle
(a) Probe clamp; (b) Calibration phantom; (c)
Schematic diagram of calibration principle

1.3 Transformation relationship between magnetic positioning space and MRI image space coordinates

In order to solve the transformation matrix $T_{m\to w}$ from magnetic positioning space to MRI image space, it is necessary to obtain the feature point set of the corresponding positions in the two spaces. Therefore, we propose a registration method based on selecting coplanar MRI and TRUS image pairs. First, determine the target level of the preoperative MRI image, use the transverse screen mode of the ultrasonic probe for scanning, move the ultrasonic probe until TRUS displays the same anatomical structure as the selected MRI level, and record the TRUS image at this time and the magnetic positioning sensor data at this time. Secondly, two-dimensional rigid registration is performed for the selected MRI and TRUS image pairs:

normalized mutual information [15] is used as the registration measure, based on $f(A,B)=(H(A)+H(B))/H(A,B)$, where $H(A)$ and $H(B)$ are the entropy of images A and B to be registered, $H(A, B)$ is the joint entropy, and the gray level for calculating mutual information is set as 32; Preprocess the selected MRI and TRUS before registration, set the pixels of the non prostate region of the selected MRI image to zero according to the pre-operative MRI prostate segmentation region, intercept the image region in the TRUS image, and remove other display annotation information; the Powell optimization method is used. The step size is set to 2, the maximum number of iterations is set to 100, the error is set to 0.0001, and the penalty coefficients for the angle and translation of the transformation matrix are set to 1000 and 1. The angle parameters obtained from the placement solution are too large; in this way, the registration matrix T2D from TRUS to the selected MRI image level can be obtained. Finally, n two-dimensional coordinate points are randomly generated in TRUS image space to obtain the point set U', and the point set M' is obtained by T2D transformation to the selected MRI level image space. Convert the point sets u'and M' into 3D space to obtain the point sets U "and M", where the coordinate value of the third dimension of the U "point set is 0, and the coordinate value of the third dimension of the M" point set is the coordinate of the selected MRI layer in the direction of the entire 3D MRI image space layer. According to $m\rlap{/}{\mathscr{C}}=T_{m\to w}T_{w\to s}T_{s\to u}u\rlap{/}{\mathscr{C}}$, $T_{w\to s}$ is obtained from the recorded magnetic positioning sensor data, and $T_{s\to u}$ is obtained from the calibration process of ultrasonic probe, the conversion matrix $T_{m\to w}$ from magnetic positioning space to MRI image space can be obtained.
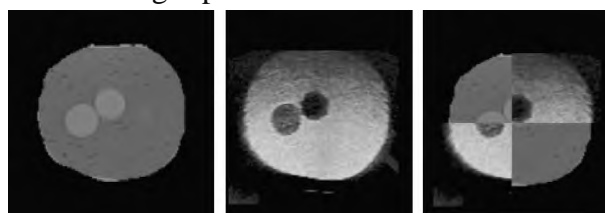

Figure 3 MRI images, TRUS images and registration results

1.4 Puncture guidance

When the real-time guidance is enabled, switch the ultrasonic probe to the sagittal scanning mode. At any time, convert the current TRUS imaging plane to MRI image space according to $m = T_{m\neg w}T_{w\neg s}T_{s\neg u}u$, and calculate the MRI re section image corresponding to the current TRUS. Similarly, the focus segmentation area of MRI image is re sectioned, and the focus area is displayed on the MRI re sectioned image. At the same time, the focus area is inversely converted to the TRUS image space, and displayed in the TRUS image, indicating the presence and location of the focus area in the current TRUS image. In addition, in order to show the relative position relationship between the current TRUS image plane and the three-dimensional model planned before operation, the re cut MRI image is displayed in the three-dimensional view, which can guide the user to move the ultrasonic probe more efficiently and make the focus area intersect with the TRUS image screen. When the focus area appears in the TRUS image, adjust the position of the puncture frame according to the distance between the focus and the ultrasonic probe, and puncture the needle. As the puncture needle moves in the TRUS image screen, the puncture process is completed when it is observed that the puncture needle reaches the focus area.
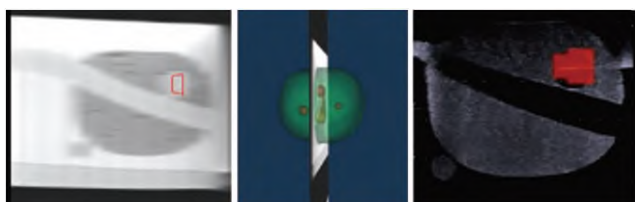
Figure 4 MRI re section images, 3D models and TRUS images in puncture guidance

1.5 System realization

The targeted puncture hardware platform consists of a computer, a magnetic locator (PA triot, Polhemus), a video capture card, a biplane intracavitary probe and a special probe fixture. The video acquisition card can intercept the screen output of the ultrasonic equipment in real time, and the special probe clamp connects the magnetic positioning sensor with the ultrasonic probe rigidly, and integrates the puncture frame function. The navigation software is developed in Visual Studio 2015 using c++ programming language, using QT, VTK, ITK and eigen toolkits. QT is used for software framework construction, VTK is used for two-dimensional and three-dimensional display of medical images, ITK is used for medical image registration, and eigen is used for matrix calculation. In addition, the prostate automatic segmentation model of MRI images is packaged into an executable program by the pyinstaller toolkit, so that the preoperative planning module of the navigation software can be called.

Figure 5 Targeted puncture system platform

2 Experimental results

In this section, the target registration error

(TRE) is used to evaluate the ultrasonic calibration error, the two-dimensional registration error between the selected MRI level and TRUS and the three-dimensional registration error. It is defined as

$$TRE\left(\boldsymbol{p}, \boldsymbol{p}'\right) = \left|\boldsymbol{Tp} - \boldsymbol{p}'\right|,$$ where p and p' are the

corresponding coordinate points under the two coordinate systems respectively, T is the conversion relationship between the two coordinate systems, and $\parallel$ represents the distance. Firstly, the verification process and calibration error of ultrasonic calibration are given, then the prostate phantom is used to verify the targeted puncture guidance method, and the registration error and puncture guidance error are calculated and evaluated. Finally, the limitations of this method are analyzed.

2.1 Ultrasonic calibration

Firstly, the accuracy of ultrasonic calibration is evaluated by experiments. Due to the use of biplane ultrasonic probe, it is necessary to calibrate the two imaging planes respectively. For each imaging plane, five pairs of TRUS images and magnetic positioning sensor data are obtained by scanning the calibration phantom. For each TRUS image, only 3 to 4 grid points closest to the probe are used to select the coordinates of grid points in the TRUS image in the software. 90% grid points are used to calculate the calibration matrix, and 10% grid points are used to verify the calibration matrix. The calibration errors of TRUS cross section and sagittal plane are 1.23 mm and 1.68 mm respectively.
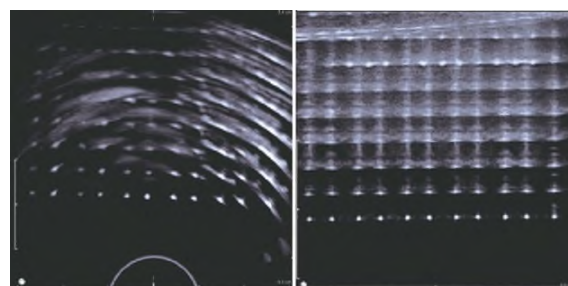

Figure 6 Ultrasonic calibration grid point image

2.2 Puncture guidance

In this study, a commercial prostate phantom (053l, CIRS, nor fold, USA) was used for experimental verification. The phantom contains simulated structures of rectal wall, prostate, urethra and seminal vesicle, as well as three simulated lesions with a diameter of about 1 cm. The phantom was scanned with a 3T MRI scanner (ingenia, Philips Medical) to obtain a T2W image with a layer thickness of 4 mm. Segment the prostate, urethra and lesion area according to the method in Section 1.1 to generate a three-dimensional model. The centers of three simulated lesions were taken as planned puncture targets, and the coordinates of puncture targets in MRI image space were recorded. Record the corresponding TRUS image and magnetic positioning sensor data according to the maximum level of the three lesions in the MRI image, and perform registration according to the method in Section 1.3.

Since the two-dimensional registration accuracy of MRI and TRUS determines the follow-up puncture guidance accuracy, the center position of the focus or urethra is selected from MRI and TRUS respectively in each group of registration. The coordinates of this position in TRUS are transformed into MRI through the two-dimensional registration matrix, and the difference calculated with the coordinates in the selected MRI is taken as the registration error. The average registration error of the six groups

is (1.91 ± 0.29) mm.

Table 1 Registration error and puncture error

Registration group	Registration error (mm)	Puncture error (mm)		
		Focus 1	Focus 2	Focus 3
1	1.62	2.14	1.79	1.57
2	1.98	1.82	1.68	2.35
3	1.52	1.67	1.83	1.71
4	1.94	1.97	1.89	1.92
5	2.19	2.36	1.95	2.05
6	2.23	2.23	2.19	2.58

After each group of image pairs were registered, puncture experiments were performed on three simulated lesions according to the method in section 1.4, and a total of 18 puncture experiments were performed. During each puncture, ensure that the current TRUS shows the largest lesion area. Because the puncture needle can be directly observed in the imaging plane of the TRUS sagittal plane, and the position of the puncture needle path can be adjusted, it can ensure that the puncture needle can accurately reach the center of the focus area in the current TRUS plane. Therefore, we recorded the TRUS image coordinates of the focus center of the TRUS image and transformed them into the MRI image space. The difference between the TRUS image coordinates and the planned coordinates of the focus center in the MRI image space was calculated as the current puncture error. The puncture error is shown in Table 1. The average error between the planned puncture point and the actual puncture point is (1.98 ± 0.28) mm.

2.3 Limitations

The above results prove that this study has achieved good performance in ultrasonic calibration and puncture guidance, but there are also some limitations. Firstly, the accuracy of ultrasonic calibration needs to be further improved. Reference [9] reports that the calibration error is less than 1 mm, which is better than the results shown in this paper. This shows that if the calibration simulator can be constructed more accurately, it is possible to control the calibration error below 1 mm, so as to further reduce the system error. Secondly, although this method does not need to establish the spatial conversion relationship between preoperative MRI and intraoperative 2D TRUS through 3D TRUS, it needs to manually select the MRI and TRUS image pairs in the same plane. If the selected images have obvious deviation, it will lead to obvious puncture guidance error. Therefore, professional clinical students need to complete the selection of image pairs. Finally, because more deformation and motion interference will be introduced into the practical clinical application, the method in this paper also needs to be verified by clinical experiments.

3 Conclusion

This paper presents an MRI-TRUS fusion method for prostate targeted puncture navigation. Based on the selected MRI-TRUS image pair, the spatial position relationship between preoperative MRI and intraoperative 2D TRUS is directly established, the real-time re section image of preoperative MRI and the real-time relative position relationship with the preoperative planning 3D model are displayed, and the focus area is mapped into trus, so as to guide the prostate targeted puncture. In this paper, the feasibility of this method is preliminarily verified by prostate phantom experiment. In the future, we will improve the calibration of phantom structure, registration method, motion compensation and other aspects to further improve the accuracy and stability of the targeted puncture navigation method, which

will be verified in clinical experiments.

References

[1] Del Monte M, Leonardo C, Salvo V, et al. MRI/US fusion-guided biopsy: performing exclusively targeted bi-opsies for the early detection of prostatecancer[J]. La Radiologia Medica, 2018, 123(3) : 227-234.

[2] Liau J, Goldberg D, Arif-Tiwari H. Prostate cancer detec-tion and diagnosis: role of ultrasound with MRI correlates [J]. Current Radiology Reports, 2019, 7(3) : 7.

[3] Deng Yisen, He Yuhui, Zhou Xiaofeng. Development of prostate targeted puncture technology[J]. Journal ofmini-mally Invasive Urology, 2018, 7(6) : 428-432.

[4] Hu Y, Ahmed H U, Taylor Z, et al. MR to ultrasound reg-istration for image-guided prostateinterventions [J]. Medical Image Analysis, 2012, 16(3) : 687-703.

[5] Wang Y, Cheng J Z, Ni D, et al. Towards personalized statistical deformable model and hybrid point matching for robust MR-TRUS registration[J]. Ieeetransactions on Medical Imaging, 2015, 35(2) : 589-604.

[6] Congming, Wu Tong, Liu Dong, et al. Prostate MR/TRUS segmentation and registration based on supervised learning[J]. Journal of Engineering Sciences, 2020, 42 (10) : 1362-1371.

[7] Hu Y, Modat M, Gibson E, et al. Weakly-supervised con-volutional neural networks for multimodal image registration [J]. Medical Image Analysis, 2018, 49: 1-13.

[8] Sheng X, Kruecker J, Turkbey B, et al. Real-time MRI-TRUS fusion for guidance of targeted prostate biopsies[J]. Computer Aided Surgery Official Journal of the International Society for Computer Aided Surgery, 2008, 13(5) : 255.

[9] Ni Dong, Wu Hailang. MRI-TRUS multi-modality image fusion for targeted prostate biopsy[J]. Journal of Shenzhen University Science and Engineering, 2016, 33(2) : 111-118.

[10] Martin P R, Cool D W, Fenster A, et al. A comparison of prostate tumor targeting strategies using magnetic resonance imaging-targeted, transrectal ultrasound-guided fusion biopsy[J]. Medical Physics, 2018, 45 (3) : 1018-1028.

[11] Hu Y, Kasivisvanathan V, Simmons L A M, et al. Devel-opment and phantom validation of a 3-D-ultrasound-guided system for targeting MRI-visible lesions during transrectal prostate biopsy[J]. IEEE Transactions on Bio-medical Engineering, 2016, 64(4) : 946-958.

[12] Milletari F, Navab N, Ahmadi S A. V-net: Fully convo-lutional neural networks for volumetric medical image seg-mentation[C]//2016 Fourth International Conference on 3D Vision (3DV). IEEE, 2016: 565-571.

[13] Mercier L, Lang□T, Lindseth F, et al. A review of cali-bration techniques for freehand 3-D ultrasound systems [J]. Ultrasound in Medicine & Biology, 2005, 31(4) : 449-471.10.

[14] Eggert D W, Lorusso A, Fisher R B. Estimating 3-D rigid body transformations: a comparison of four major algorithms[J]. Machine Vision and Applications, 1997, 9(5) : 272-290.11.

[15] Gong L, Wang H, Peng C, et al. Non-rigid MR-TRUS image registration for image-guided prostate biopsy using correlation ratio-based mutualinformation[J]. Biomedical Engineering Online, 2017, 16(1) : 1-21.